

TQCD Meeting 18/1/2022 @ AS

Kaon PDFs

Wen-Chen Chang

January 18th, 2022

In collaboration with

Chia-Yu Hsieh, Yu-Shiang Lian, Jen-Chieh Peng,

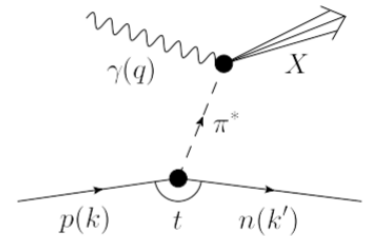
Stephane Platchkov and Takahiro Sawada

Outline

- Recent results of pion PDFs
- Data related to the kaon PDFs
- Simple phenomenology studies about kaon PDFs
- Recent theoretical results of kaon PDFs
- Future experimental programs related to kaon PDFs

Experimental Approaches of Accessing Pion Structure

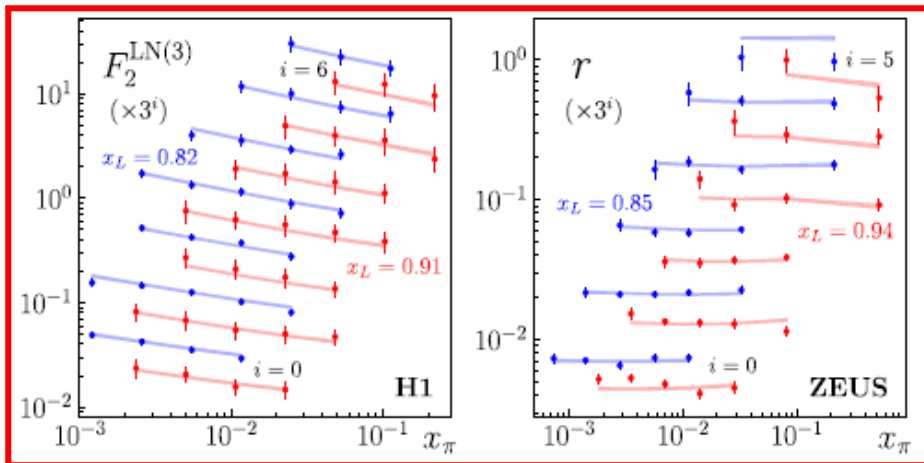
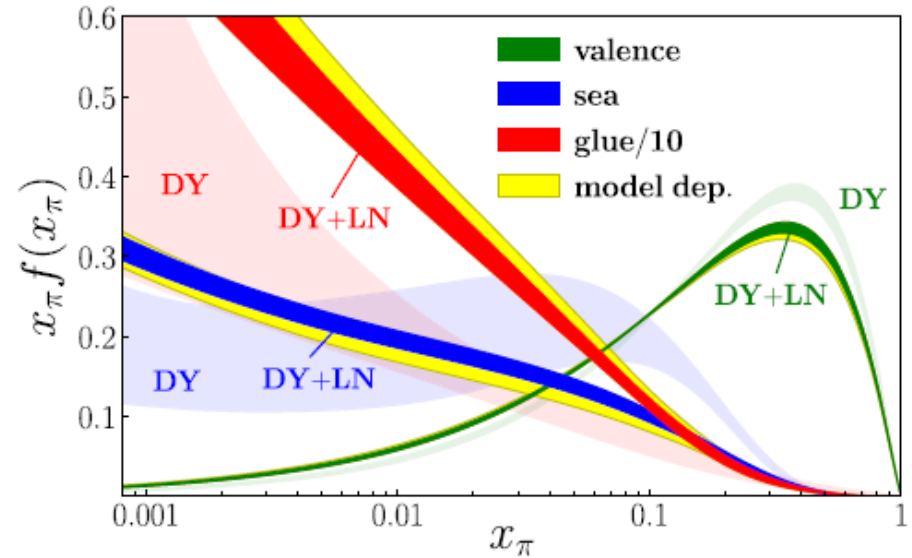
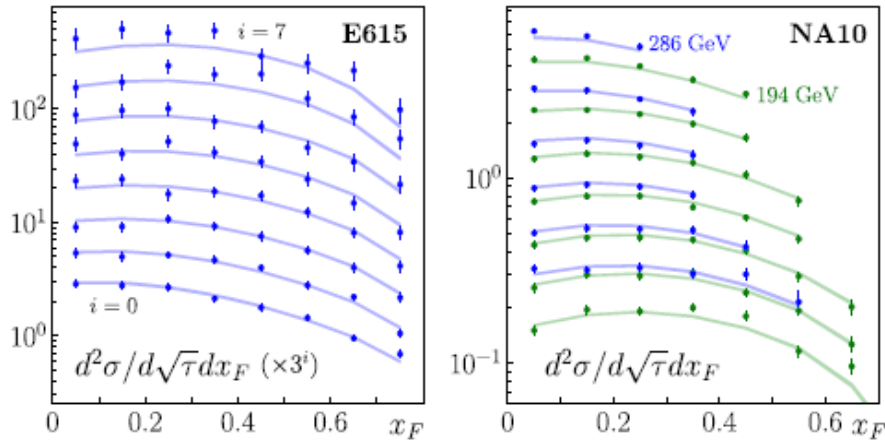
- Drell-Yan: $\pi^\pm p \rightarrow \mu^+ \mu^- X$ (LO: sensitive to valence quarks)
 - LO: $q\bar{q} \rightarrow \mu^+ \mu^-$
 - NLO: $q\bar{q} \rightarrow \mu^+ \mu^- G, qG \rightarrow \mu^+ \mu^- q$ (large p_T)
 - NNLO: $q\bar{q}G \rightarrow \mu^+ \mu^- G, qG \rightarrow \mu^+ \mu^- qG, GG \rightarrow \mu^+ \mu^- q\bar{q}$
- Direct photon: $\pi^\pm p \rightarrow \gamma X$ (LO: sensitive to gluons)
 - LO: $q\bar{q} \rightarrow \gamma G, qG \rightarrow \gamma q$
- Jpsi: $\pi^\pm p \rightarrow J/\psi X$ (LO: sensitive to gluons)
 - LO: $q\bar{q} \rightarrow c\bar{c} \rightarrow J/\psi X, GG \rightarrow c\bar{c} \rightarrow J/\psi X$
 - NLO: $q\bar{q} \rightarrow c\bar{c}G \rightarrow J/\psi X, GG \rightarrow c\bar{c}G \rightarrow J/\psi X, qG \rightarrow c\bar{c}q \rightarrow J/\psi X$
- Leading neutron (LN) electroproduction:
Sullivan processes from a nucleon's pion cloud



Pion PDFs (2021)

PDF	DY (xF, pT)	Direct γ	J/ψ	LN	Refs.
OW	*		*		PRD 1984
ABFKW	*	*			PLB 1989
SMRS	*	*			PRD 1992
GRV	*	*			ZPC 1992
GRS	*				EPJC 1999
JAM18	*			*	PRL 2018
BS, BBP	*				NPA 2019 PLB 2021
xFitter	*	*			PRD 2020
JAM21	*			*	PRD 2021 PRL 2021

JAM18: Include leading neutron (LN) electroproduction from HERA [Barry et al., PRL 121, 152001 (2018)]



- Uncertainties are much reduced using DY+LN, as compared to DY alone.

JAM21: finite q_T

[Cao et al., PRD 103, 114014 (2021)]

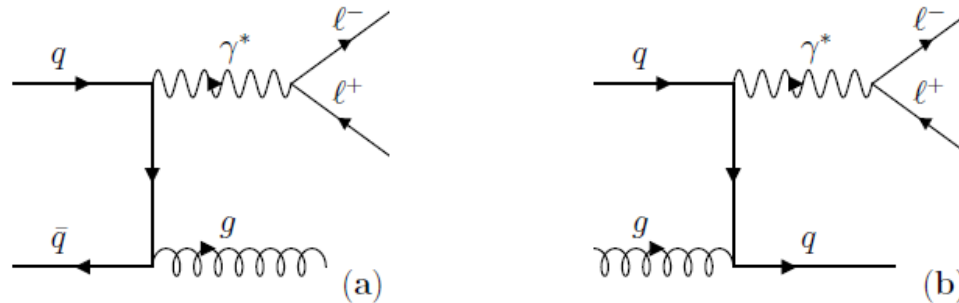


FIG. 1. Examples of LO diagrams for the large transverse momentum region in Drell-Yan lepton-pair production for the $q\bar{q}$ channel (a) and qg channel (b).

$H_{a,b}^{\text{DY}}$ starts at $\mathcal{O}(\alpha_s^0)$, and in our analysis we compute corrections up to $\mathcal{O}(\alpha_s)$. Our study is the first attempt to include both p_T -differential and p_T -integrated pion-nucleus Drell-Yan data [4, 5] on the same footing, taking advantage of the fact that the p_T -dependent cross sections provide access to a larger region of parton momentum fractions relative to the p_T -integrated case.

JAM21: Threshold Resummation

[Barry et al., PRL 127, 232001 (2021)]

$$(1-x)^{\beta_v^{\text{eff}}}$$

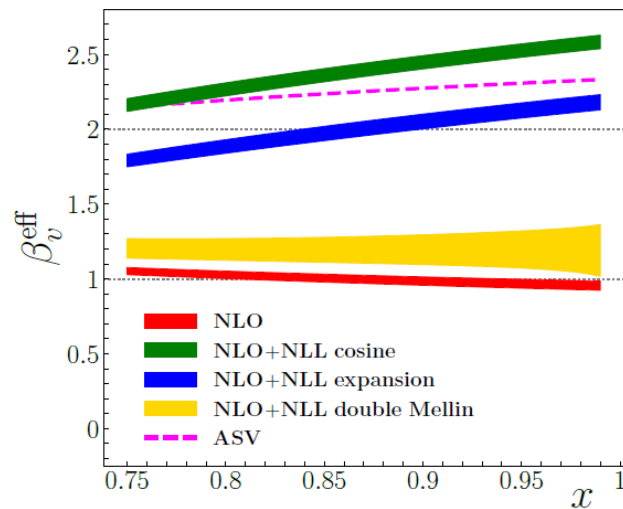


FIG. 3. Effective exponents β_v^{eff} for the various prescriptions versus x at the scale μ_0 , compared with the ASV extraction [33]. The values $\beta_v^{\text{eff}} = 1$ and 2 are shown for reference.

results in a wide variety of β_v^{eff} values, with the cosine and expansion methods yielding $\beta_v^{\text{eff}} > 2$, consistent with ASV [33], and as large as ≈ 2.6 . However, with the double Mellin method the effective exponent is much closer to the NLO case, with $\beta_v^{\text{eff}} \approx 1.2$ as $x \rightarrow 1$. This suggests that with currently available data and theoretical methods, we cannot distinguish between $\beta_v^{\text{eff}} \sim 1$ and ~ 2 asymptotic behaviors.

Large systematics of threshold resummation prescriptions!

JAM21: Momentum Fractions

[Barry et al., PRL 127, 232001 (2021)]

TABLE II. Momentum fractions of the pion carried by valence quarks, sea quarks and gluons at the input scale, $\mu^2 = m_c^2$, and at $\mu^2 = 10 \text{ GeV}^2$, for various combinations of data sets used in this analysis. The results for the full analysis (“DY+LN+DY p_T ”) are given in boldface.

data sets	$\mu^2 = m_c^2$			$\mu^2 = 10 \text{ GeV}^2$		
	$\langle x \rangle_v^\pi$	$\langle x \rangle_s^\pi$	$\langle x \rangle_g^\pi$	$\langle x \rangle_v^\pi$	$\langle x \rangle_s^\pi$	$\langle x \rangle_g^\pi$
DY	0.59(1)	0.28(10)	0.13(11)	0.49(1)	0.26(8)	0.25(8)
DY+LN	0.53(2)	0.14(4)	0.34(6)	0.43(2)	0.17(3)	0.40(4)
DY+LN+DY p_T	0.54(2)	0.16(3)	0.29(5)	0.44(1)	0.19(2)	0.37(3)

TABLE I. Total momentum fractions of the valence quark, sea quark, and gluon distributions at the input scale $\mu = \mu_0$ for various resummation prescriptions.

resummation method	$\langle x \rangle_v$	$\langle x \rangle_s$	$\langle x \rangle_g$
NLO	0.53(2)	0.14(4)	0.34(6)
NLO+NLL cosine	0.47(2)	0.14(5)	0.39(6)
NLO+NLL expansion	0.46(2)	0.16(5)	0.38(6)
NLO+NLL double Mellin	0.46(3)	0.15(7)	0.40(5)

the double Mellin resummation favors a larger gluon at higher x

LQCD: Pion Momentum Fractions

[Alexandrou et al., PRL 127, 252001 (2021)]

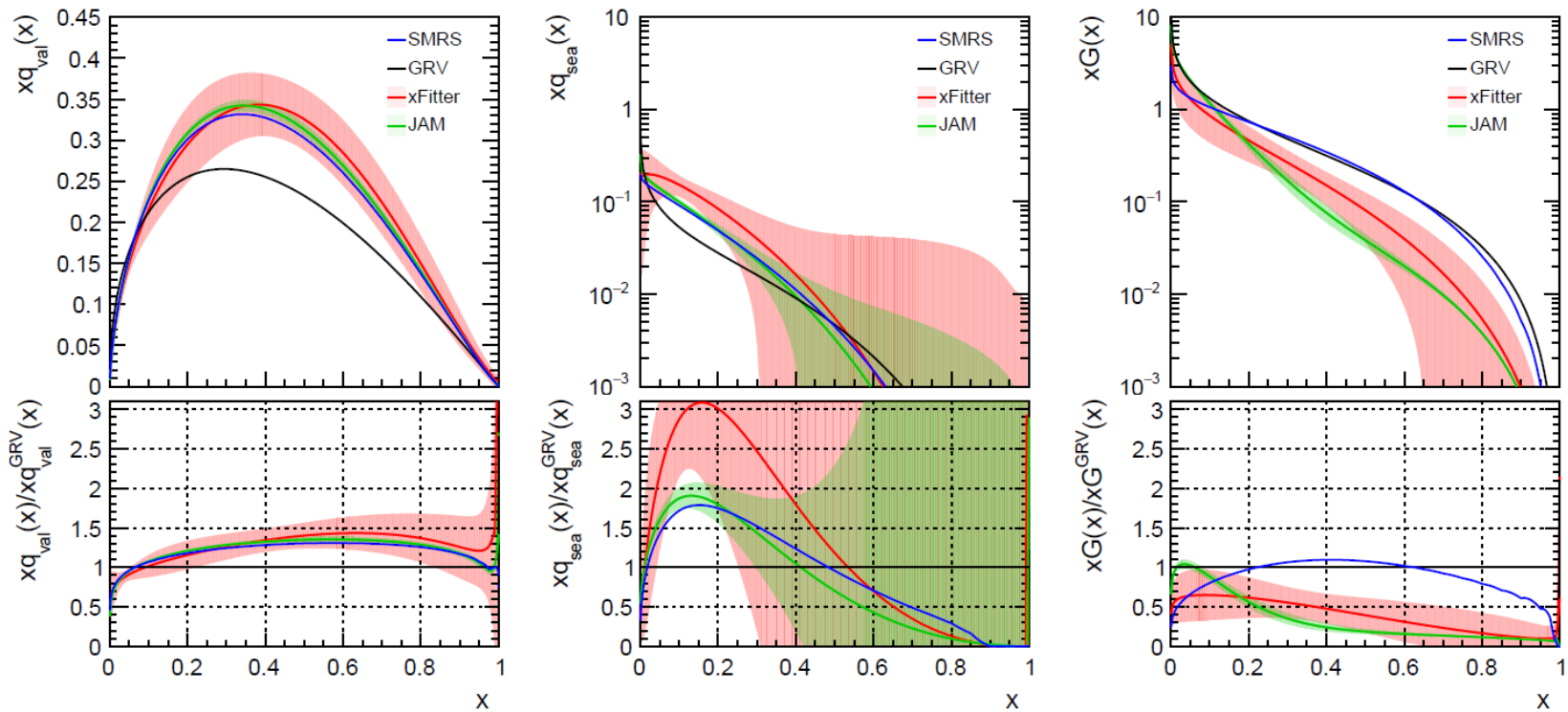
TABLE I. Compilation of results and comparison to literature. All values are at 2 GeV in the $\overline{\text{MS}}$ scheme.

	This work	RQCD [20]	JAM [45]	xFitter [46]
$\langle x \rangle_l^R$	0.601(28) ₍₋₂₁₎
$\langle x \rangle_s^R$	0.059(13) ₍₋₁₀₎
$\langle x \rangle_c^R$	0.019(05) ₍₋₁₀₎
$\langle x \rangle_g^R$	0.52(11) ⁽⁺⁰²⁾	...	0.42(4)	0.25(13)
$\sum_f \langle x \rangle_f^R$	0.68(05) ₍₋₀₃₎	0.220(207)	0.58(9)	0.75(18)
$\langle x \rangle_{u+d-2s}^R$	0.48(01)	0.344(28)
$\langle x \rangle_{u+d+s-3c}^R$	0.60(03)

The gluon momentum fraction from LQCD is larger than those of JAM and xFitter.

Pion PDFs

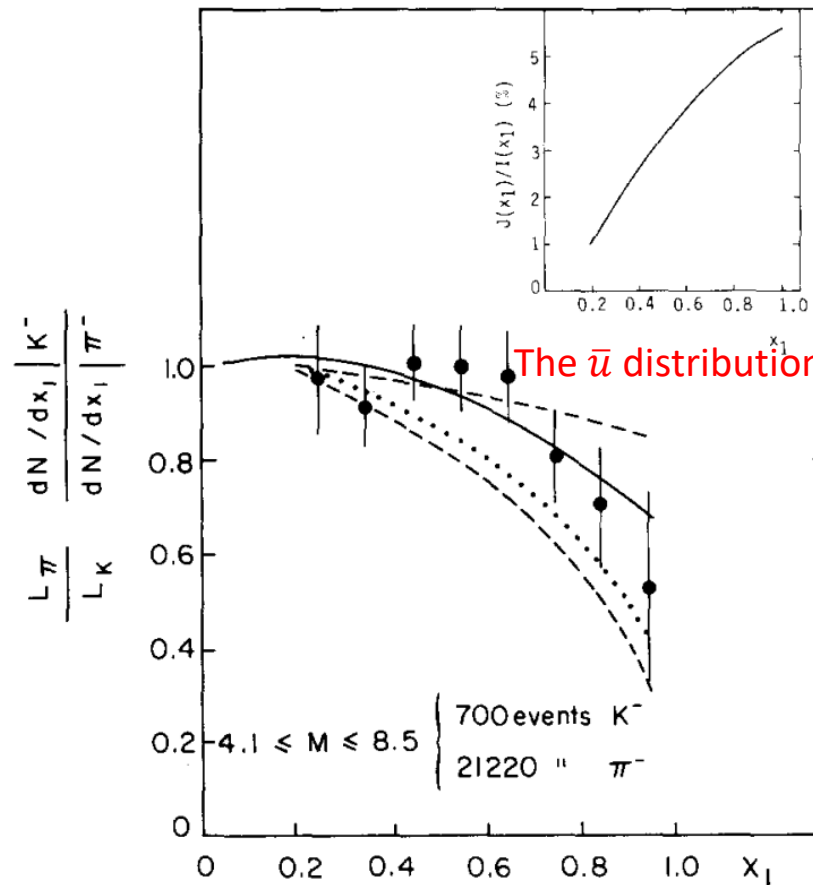
$$Q^2 = 9.6 \text{ GeV}^2$$



The gluon distributions of SMRS and GRV are significantly larger than JAM and xFitter for $x > 0.1$.

Kaon/Pion Drell-Yan Ratios

NA10: J. Badier et al., Phys. Lett. B 93, 354 (1980)

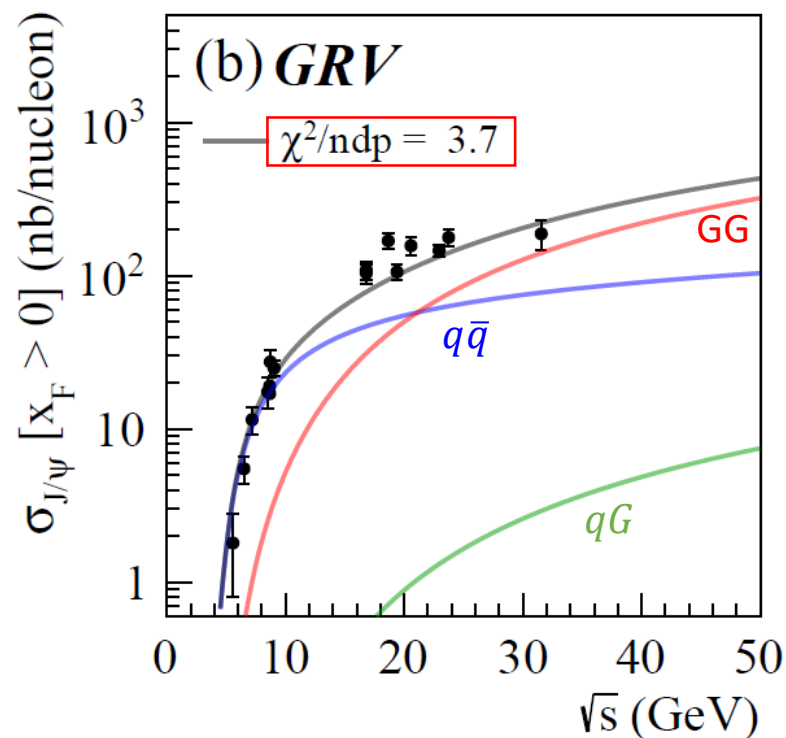
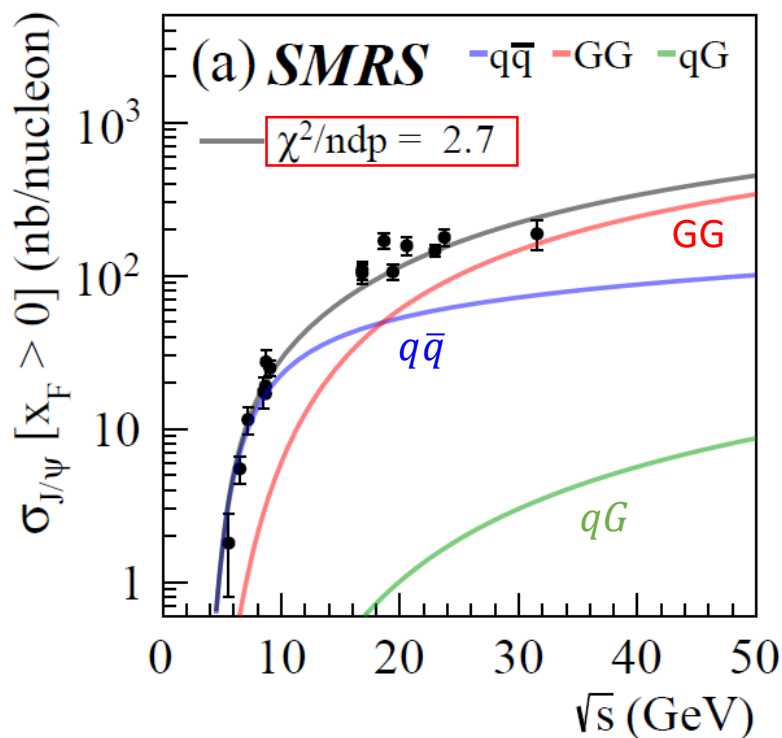


The \bar{u} distribution of kaon is softer than pion's.

$$\frac{\sigma^{DY}(K^-)}{\sigma^{DY}(\pi^-)}(x_F) = \frac{\bar{u}^K(x_1)u^N(x_2)}{\bar{u}^\pi(x_1)u^N(x_2)} = \frac{\bar{u}^K}{\bar{u}^\pi}(x_1)$$

$\pi^- + N \rightarrow J\psi + X$: pion PDFs

C.Y. Hsieh et al., Chinese Journal of Physics 73 (2021) 13; arXiv 2103.11660

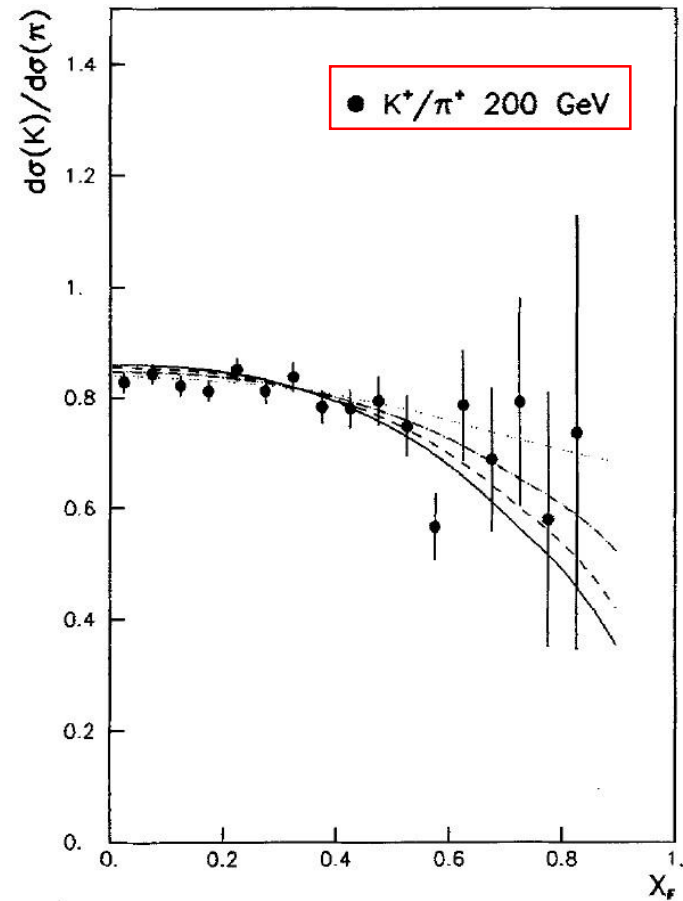
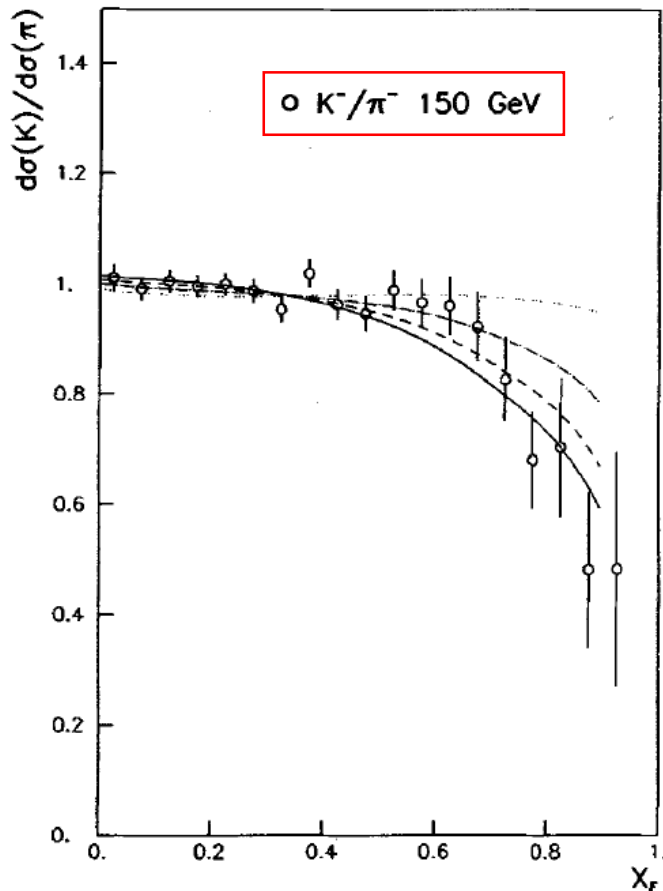


GG dominates at high energies while $q\bar{q}$ is important near threshold.

Kaon/Pion Jpsi Ratios

NA3: Z. Phys. C 20, 101 (1983)

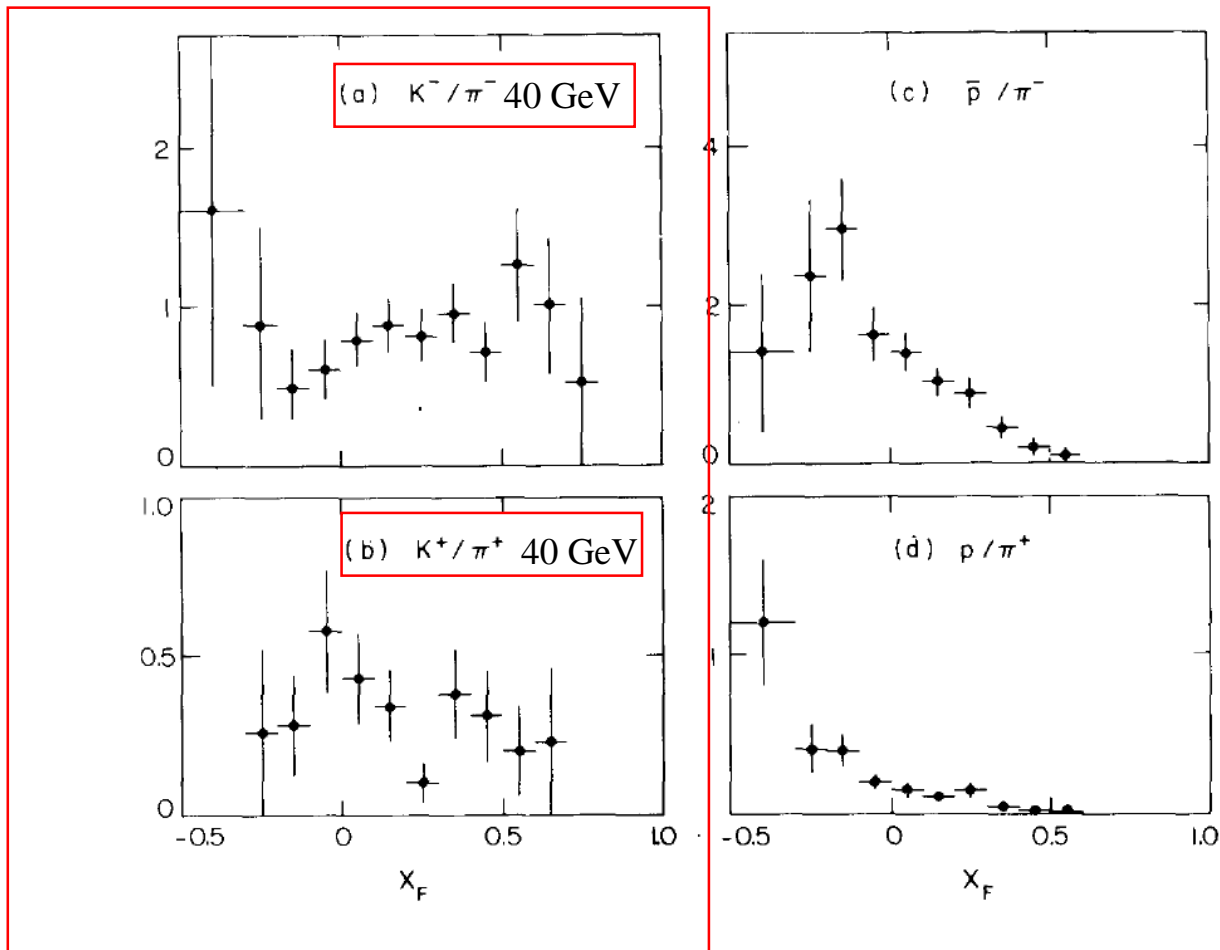
$$\frac{\sigma^{Jpsi}(K^-)}{\sigma^{Jpsi}(\pi^-)}(x_F) = \frac{\sigma(\bar{u}^K(x_1)u^N(x_2)) + \sigma(G^K(x_1)G^N(x_2))}{\sigma(\bar{u}^\pi(x_1)u^N(x_2)) + \sigma(G^\pi(x_1)G^N(x_2))} \quad \frac{\sigma^{Jpsi}(K^+)}{\sigma^{Jpsi}(\pi^+)}(x_F) = \frac{\sigma(u^K(x_1)\bar{u}^N(x_2)) + \sigma(\bar{s}^K(x_1)s^N(x_2)) + \sigma(G^K(x_1)G^N(x_2))}{\sigma(u^\pi(x_1)\bar{u}^N(x_2)) + \sigma(\bar{d}^\pi(x_1)d^N(x_2)) + \sigma(G^\pi(x_1)G^N(x_2))}$$



Kaon/Pion Jpsi Ratios

Phys. Lett. B 96, 411 (1980)

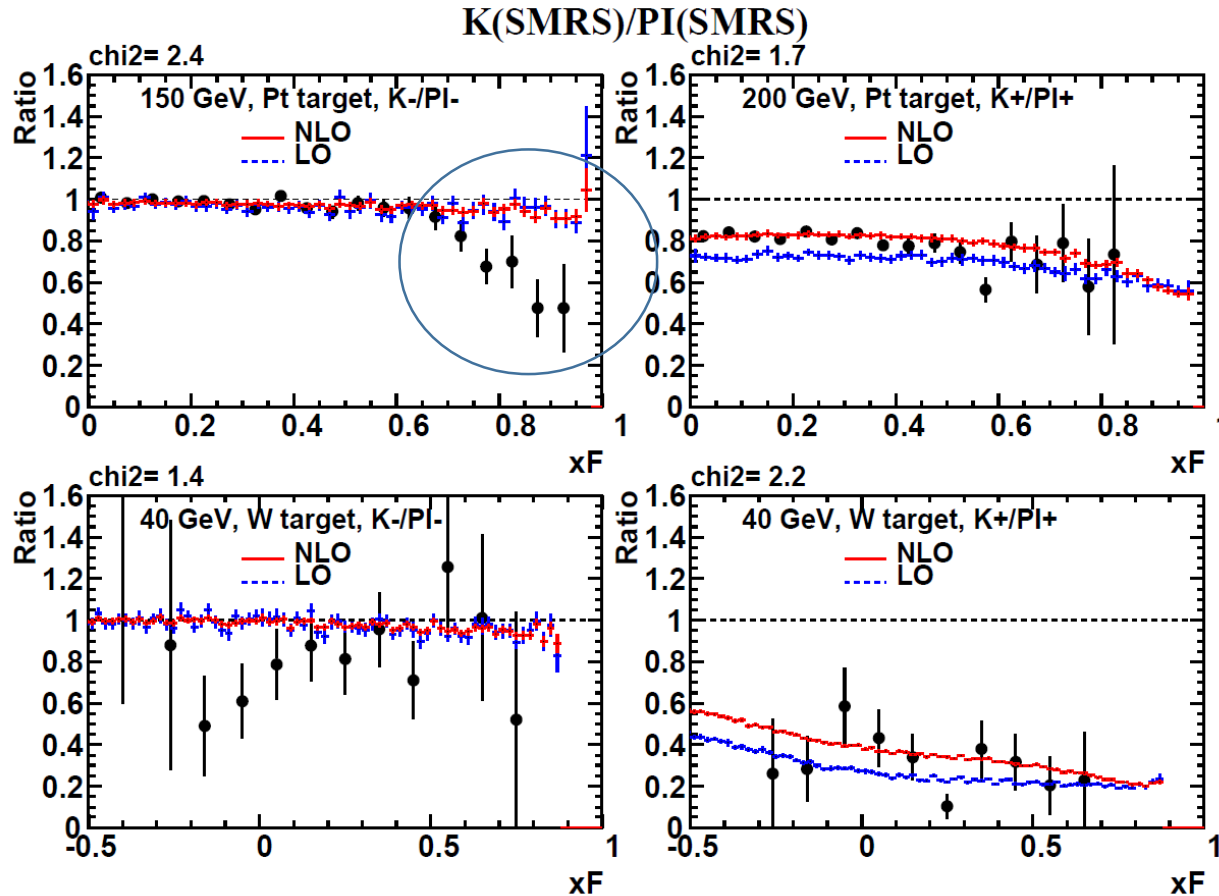
$$\frac{\sigma^{J\psi}(K^-)}{\sigma^{J\psi}(\pi^-)}(x_F) = \frac{\sigma(\bar{u}^K(x_1)u^N(x_2)) + \sigma(G^K(x_1)G^N(x_2))}{\sigma(\bar{u}^\pi(x_1)u^N(x_2)) + \sigma(G^\pi(x_1)G^N(x_2))} \quad \frac{\sigma^{J\psi}(K^+)}{\sigma^{J\psi}(\pi^+)}(x_F) = \frac{\sigma(u^K(x_1)\bar{u}^N(x_2)) + \sigma(\bar{s}^K(x_1)s^N(x_2)) + \sigma(G^K(x_1)G^N(x_2))}{\sigma(u^\pi(x_1)\bar{u}^N(x_2)) + \sigma(\bar{d}^\pi(x_1)d^N(x_2)) + \sigma(G^\pi(x_1)G^N(x_2))}$$



CEM K/pi Ratios: SMRS

Kaon PDF: Pion PDF with $d \rightarrow s$

CEM NLO results agree with the data.



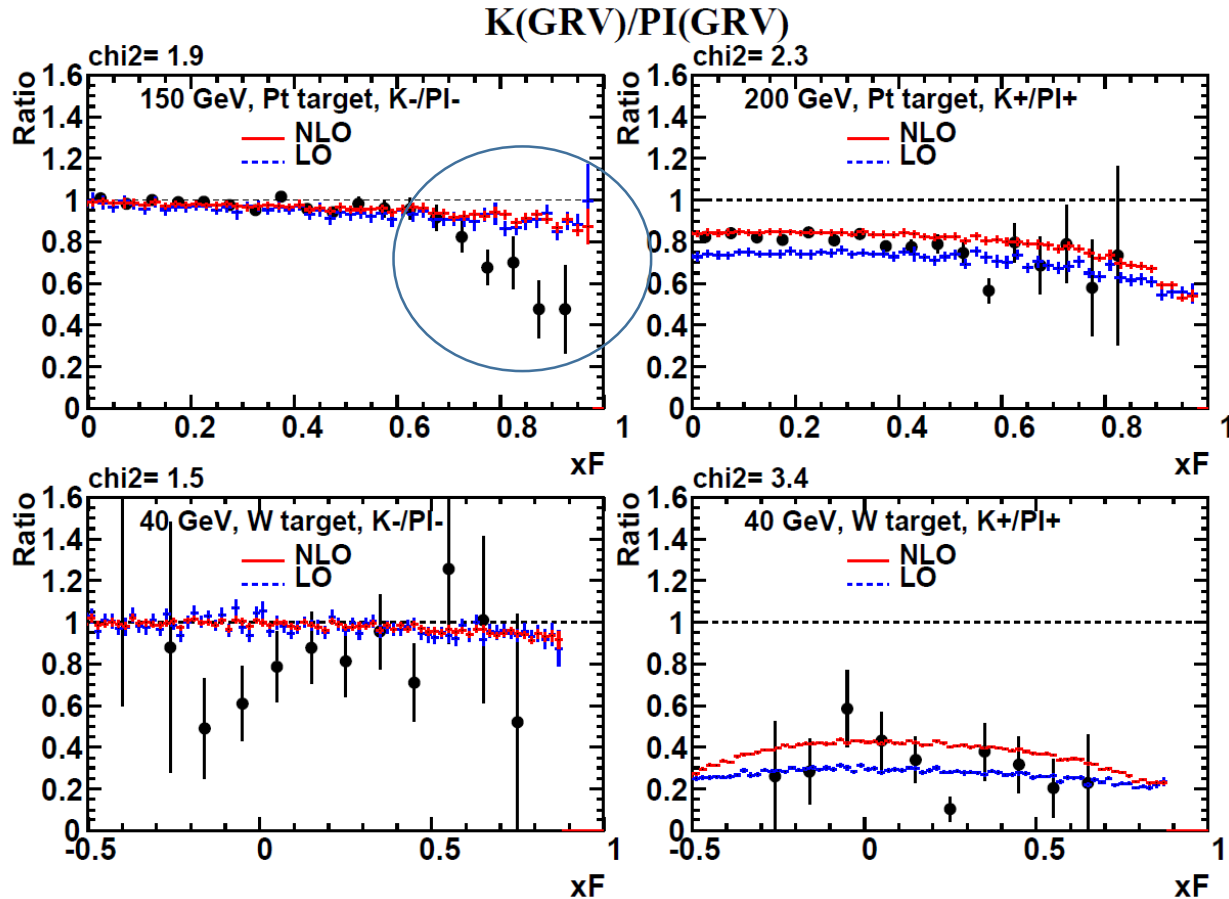
Color Evaporation Model (CEM)

W.C. Chang et al., Phys. Rev. D 102, 054024 (2020); arXiv: 2006.06947

CEM K/pi Ratios: GRV

Kaon PDF: Pion PDF with $d \rightarrow s$

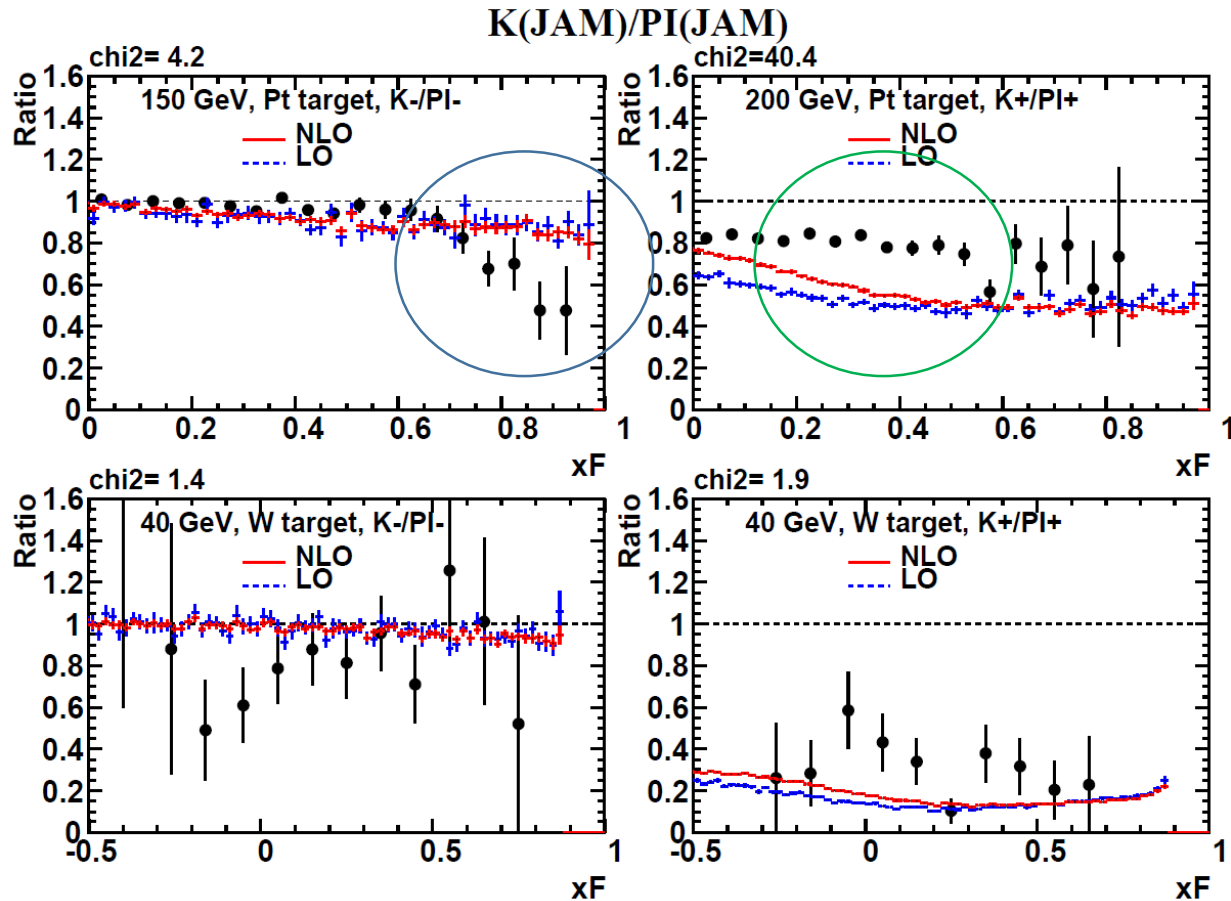
CEM NLO results agree with the data.



CEM K/pi Ratios: JAM

Kaon PDF: Pion PDF with $d \rightarrow s$

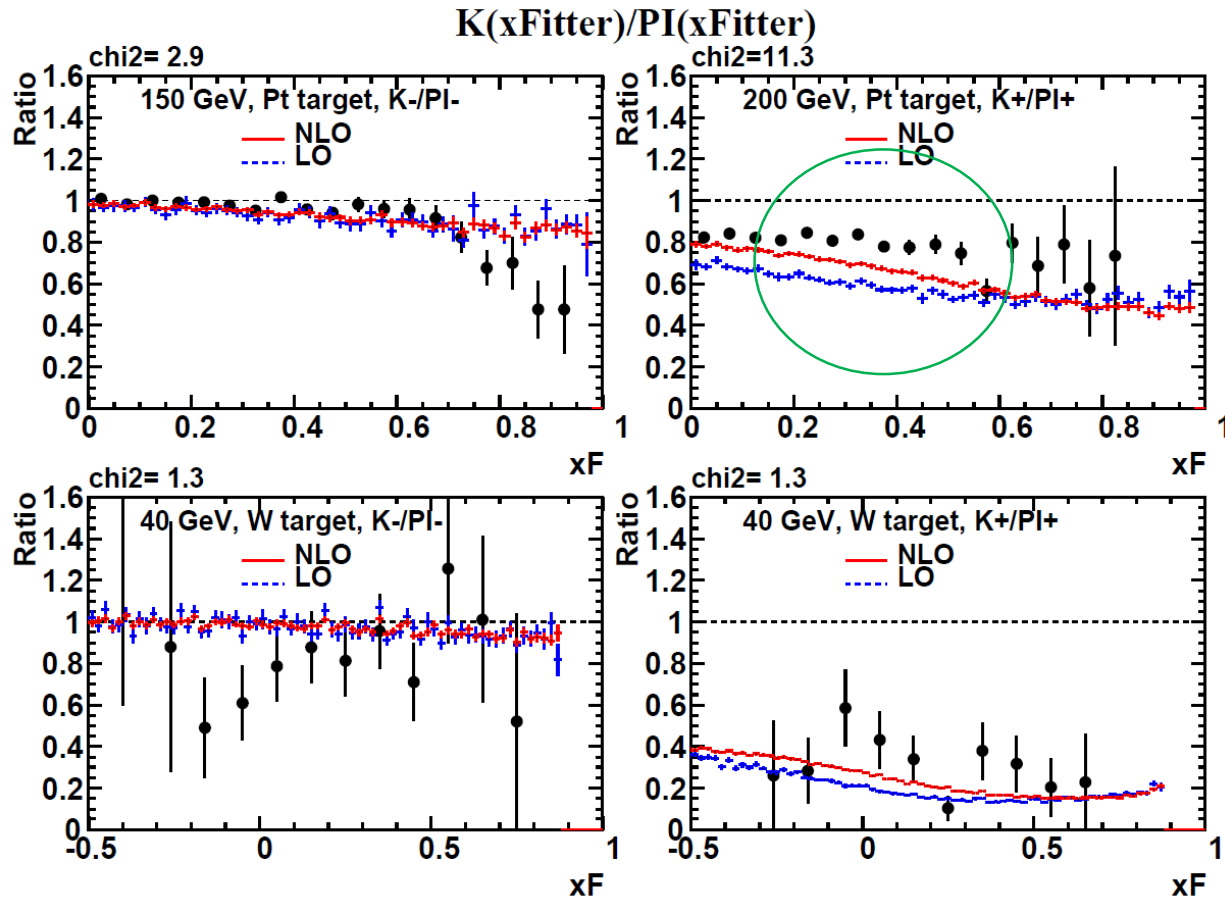
Data are under-estimated, due to weak gluon.



CEM K/pi Ratios: xFitter

Kaon PDF: Pion PDF with $d \rightarrow s$

Data are under-estimated, due to weak gluon.



(LO) NRQCD LDMEs

	qqbar	GG	qqbar	GG
LDMEs	0_8(3S1) Jpsi	0_8(1S0) Jpsi	0_8(3S1) psi'	0_8(1S0) psi'
Beneke (0)	6.6E-3	3.75E-3	4.60E-3	6.50E-4
SMRS (1)	6.3E-2	3.63E-3	2.02E-2	2.01E-4
GRV (2)	8.9E-2	3.11E-3	2.56E-2	1.15E-4
JAM (3)	9.3E-2	9.75E-4	2.28E-2	1.15E-8
xFitter (4)	7.3E-2	2.83E-3	2.37E-2	1.67E-4

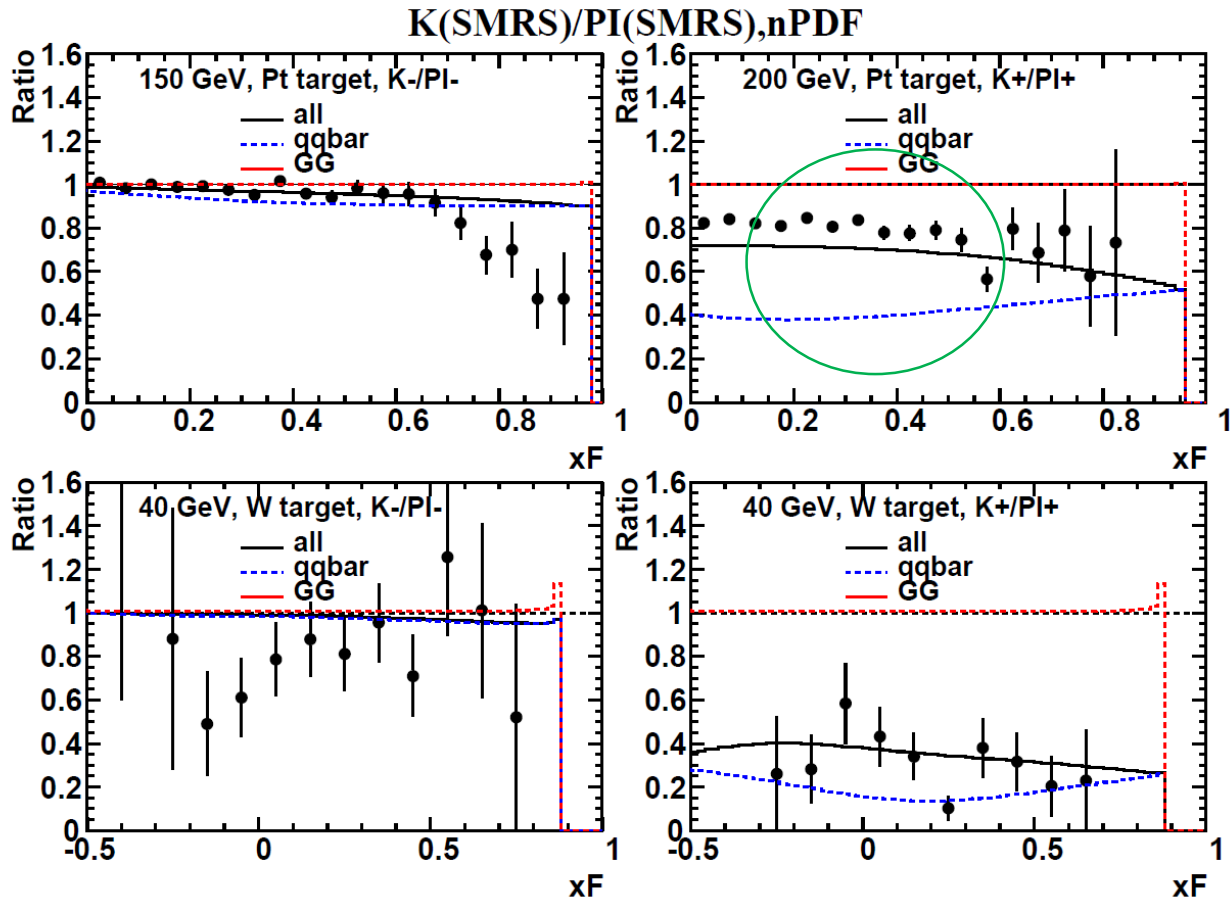
NRQCD

C.Y. Hsieh et al., Chinese Journal of Physics 73 (2021) 13; arXiv 2103.11660

NRQCD K/pi Ratios: SMRS

Kaon PDF: Pion PDF with $d \rightarrow s$

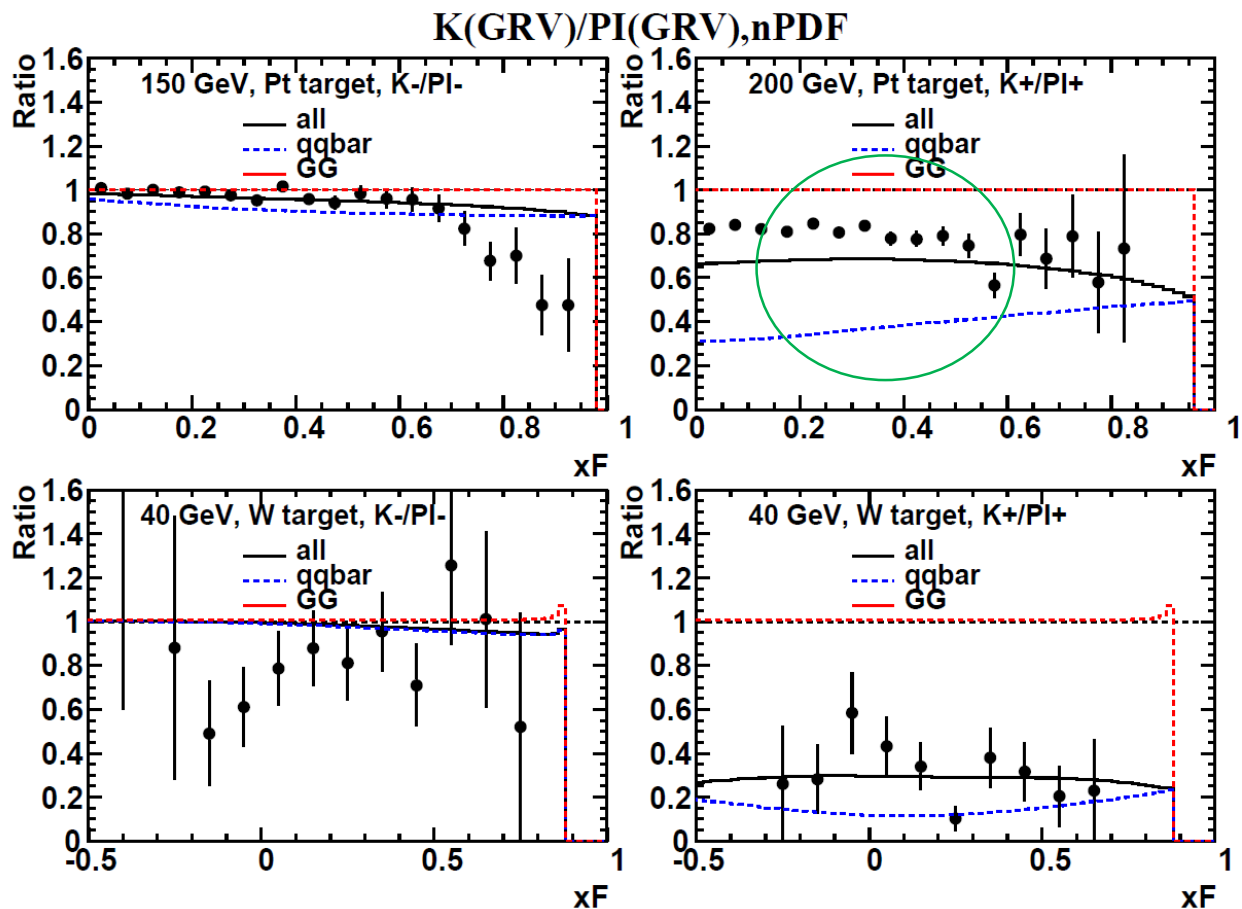
Glucan strength in kaon is not large enough.



NRQCD K/pi Ratios: GRV

Kaon PDF: Pion PDF with $d \rightarrow s$

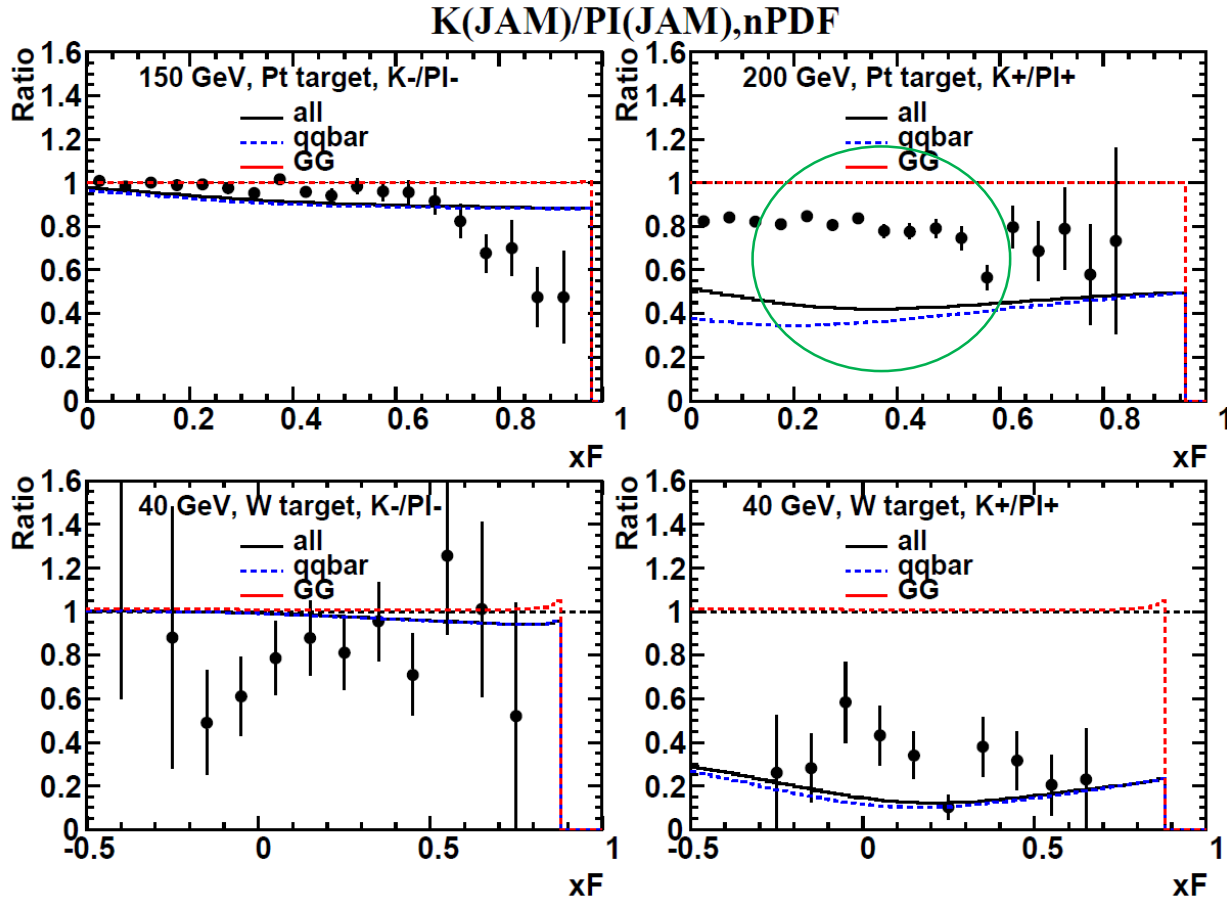
Glucan strength in kaon is not large enough.



NRQCD K/pi Ratios: JAM

Kaon PDF: Pion PDF with $d \rightarrow s$

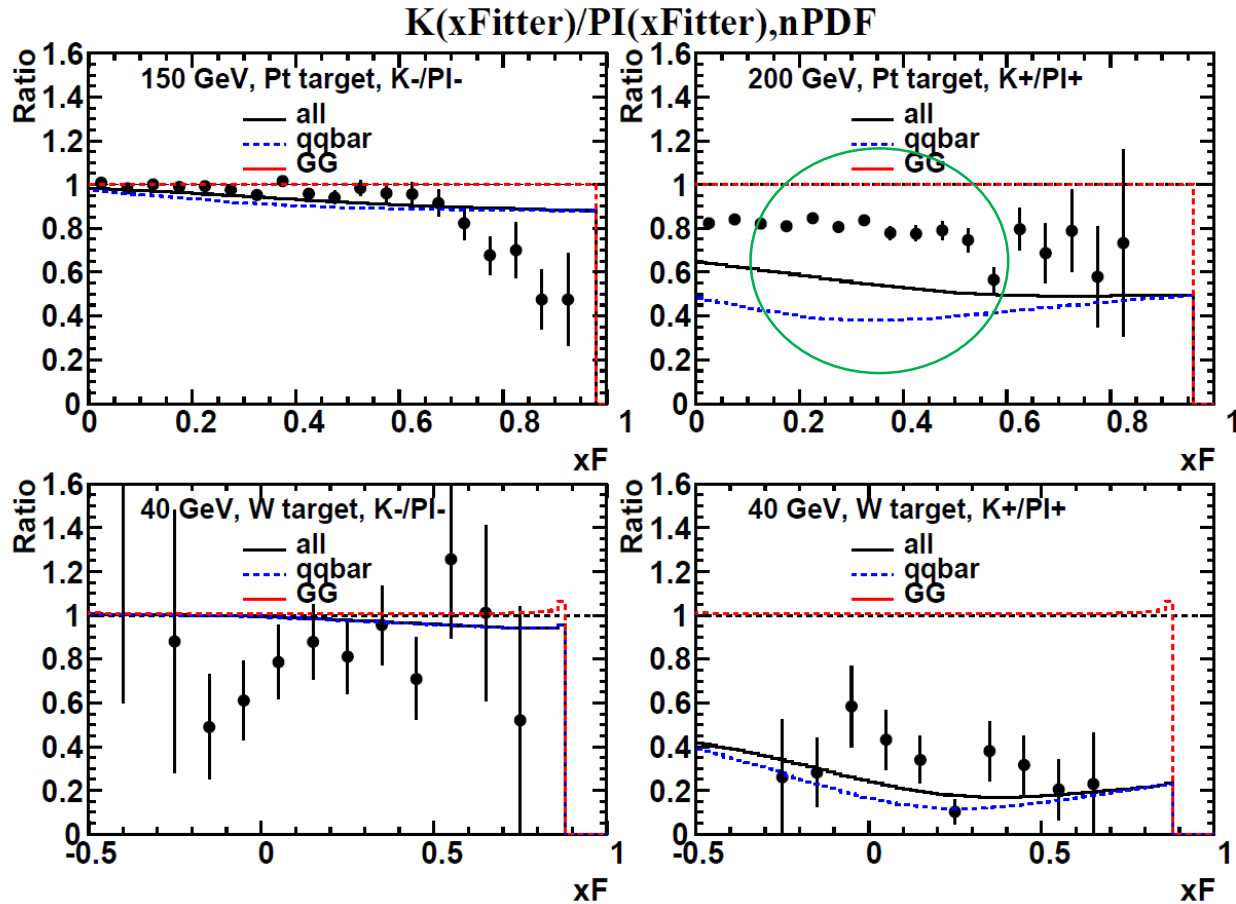
Glucan strength in kaon is not large enough.



NRQCD K/pi Ratios: xFitter

Kaon PDF: Pion PDF with $d \rightarrow s$

Glucan strength in kaon is not large enough.

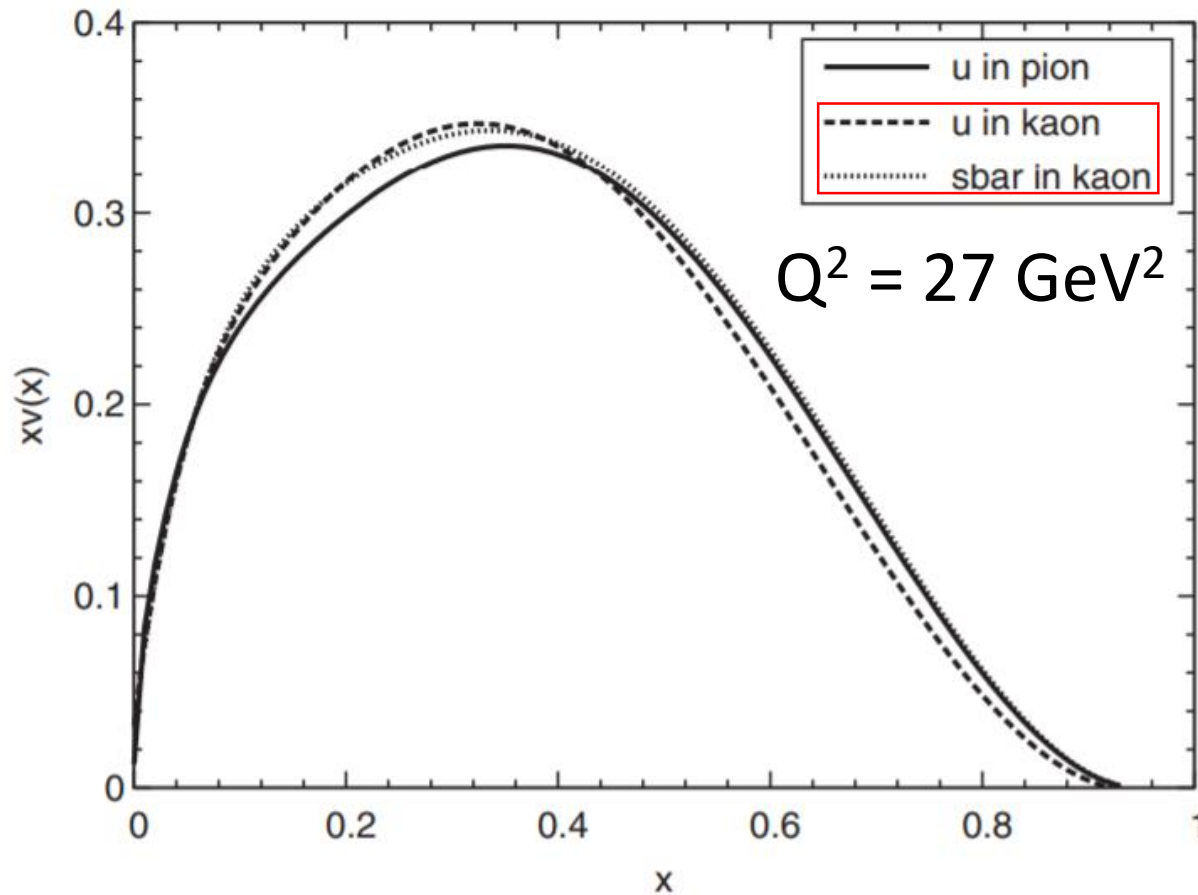


Observations

- The large- x gluon strength of kaons might be equal (CEM) or slightly stronger (NRQCD) than that of pions.
- The large- x gluon strengths of xFitter and JAM pion PDFs seem too weak to describe both data sets of pion- and kaon-induced J/ψ production.

Kaon PDFs: chiral constituent quark model

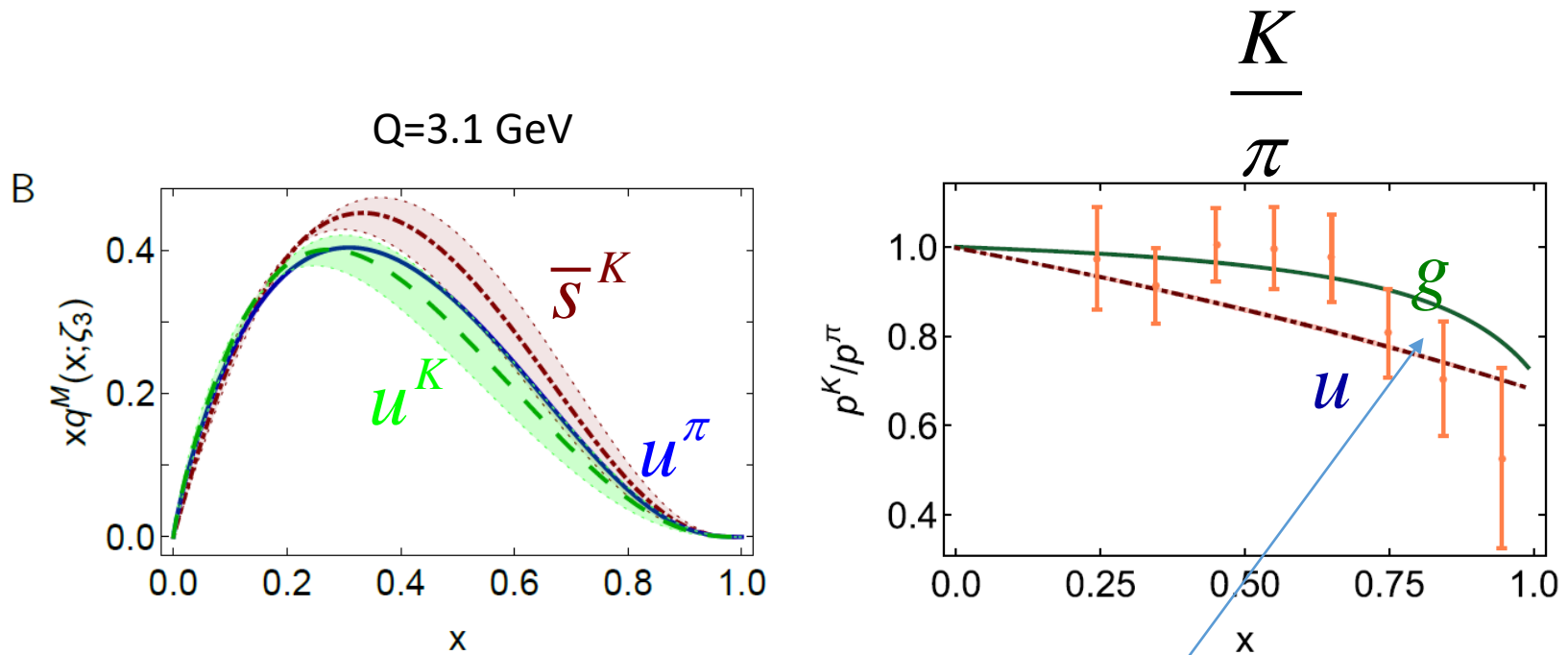
PRD 97, 074015 (2018)



A small SU(3) flavor symmetry breaking effect

Kaon PDFs: Dyson-Schwinger Equation (DSE)

Eur. Phys. J. C (2020) 80:1064

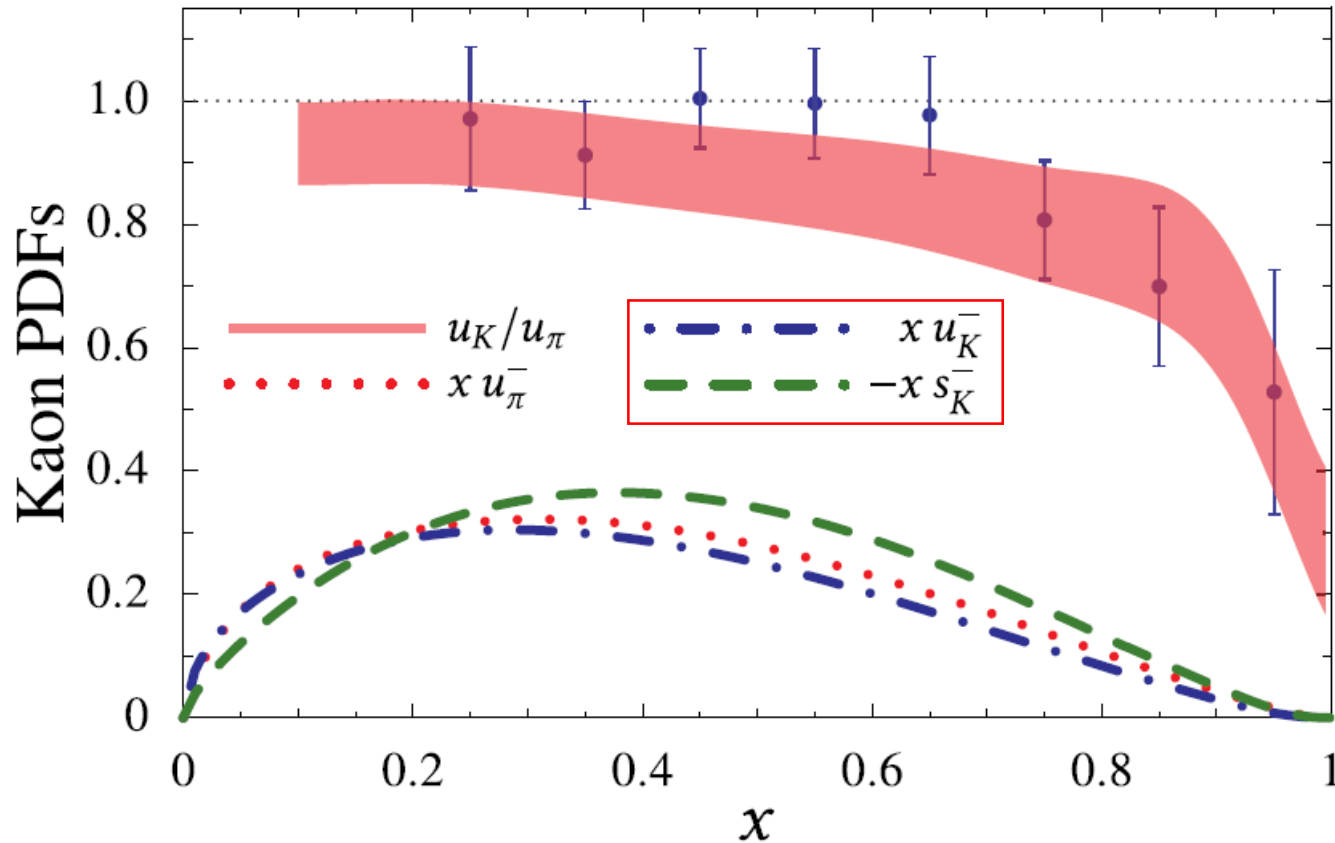


$$\langle x[2u^\pi(x; \zeta_3) + g^\pi(x; \zeta_3) + S^\pi(x; \zeta_3)] \rangle = 1.$$

A slightly smaller kaon gluon distribution at large x , compared to the pion.

Kaon PDFs: Dyson-Schwinger Equation (DSE)

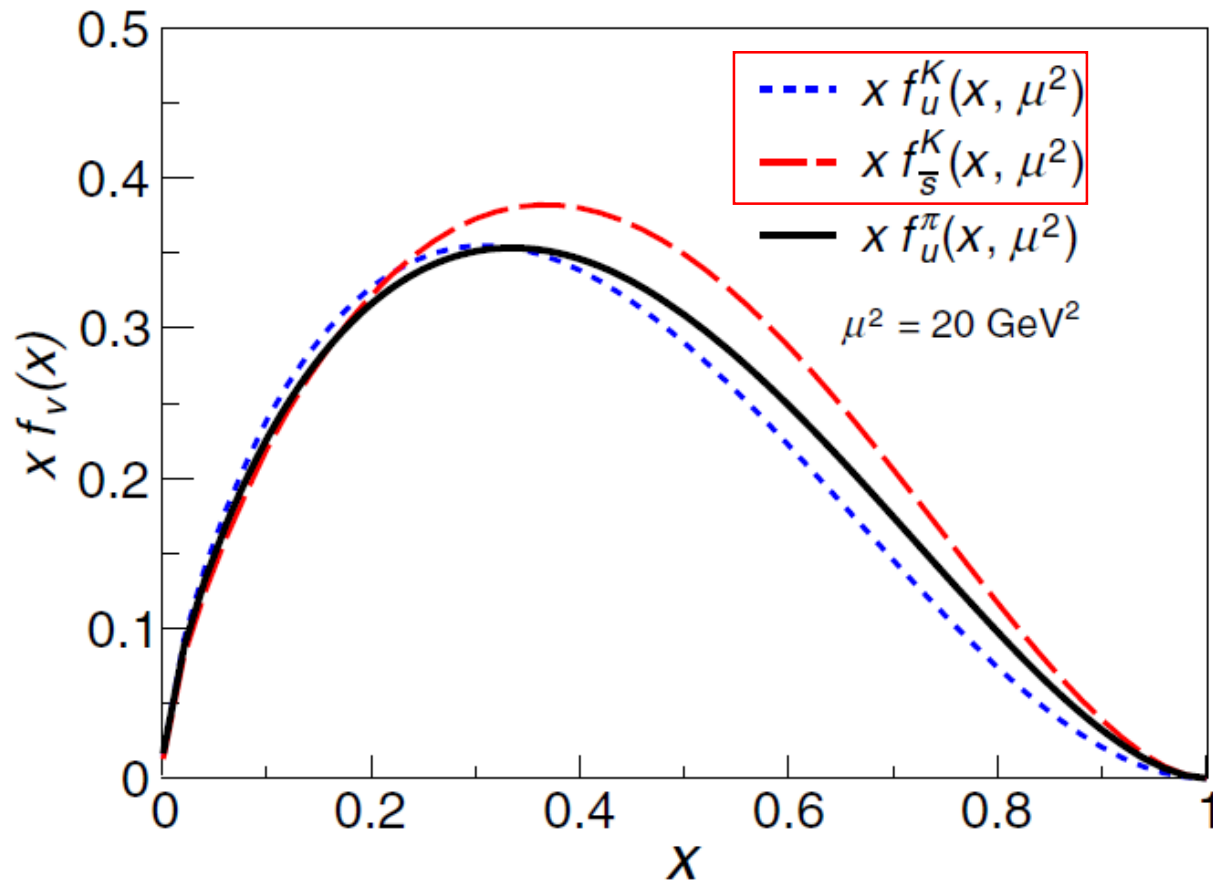
PRL 124, 042002 (2020)



region. An immediate consequence of this nonperturbative gluon dressing is that gluons carry 35% of the pion's and 30% of the kaon's light-cone momentum at the initial scale of the DSE calculations. Our results for the pion and kaon

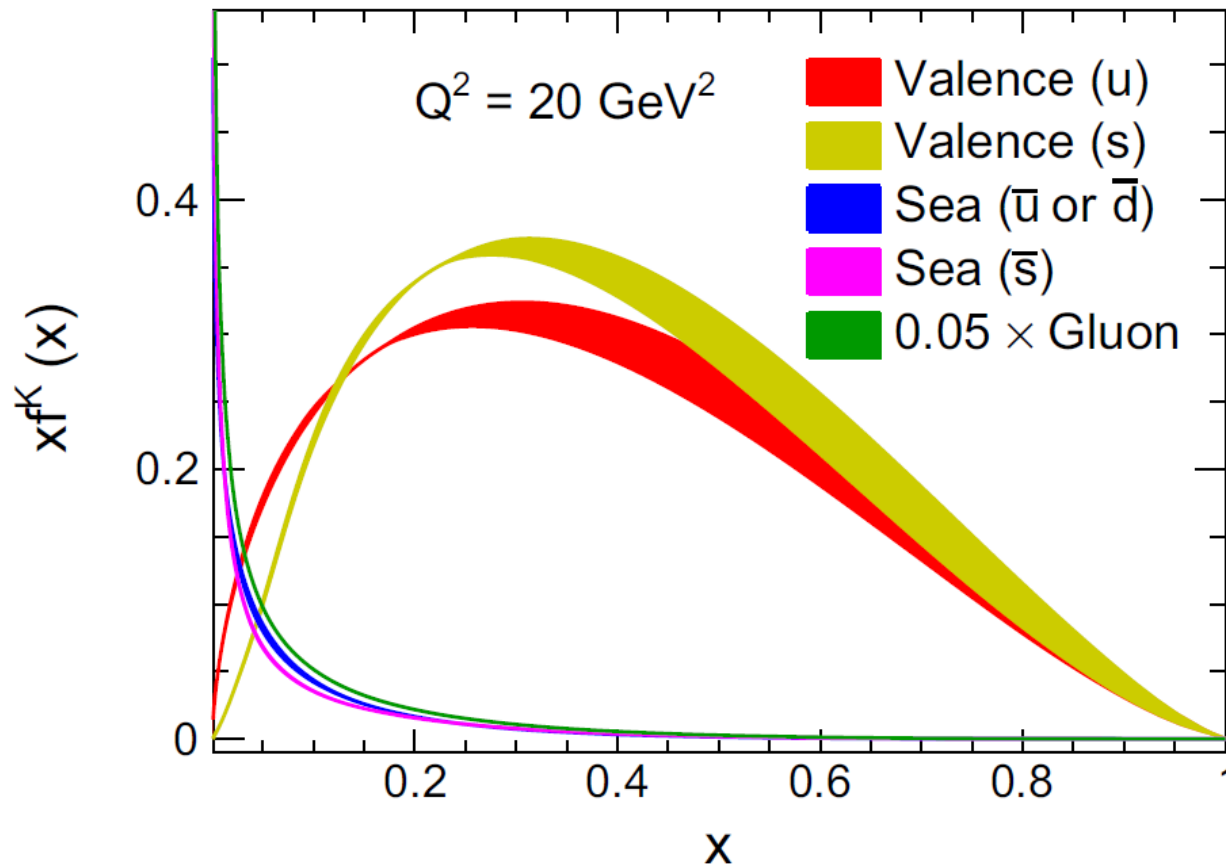
Kaon PDFs: Light-Front Quantization

PRD 101, 034024 (2020)



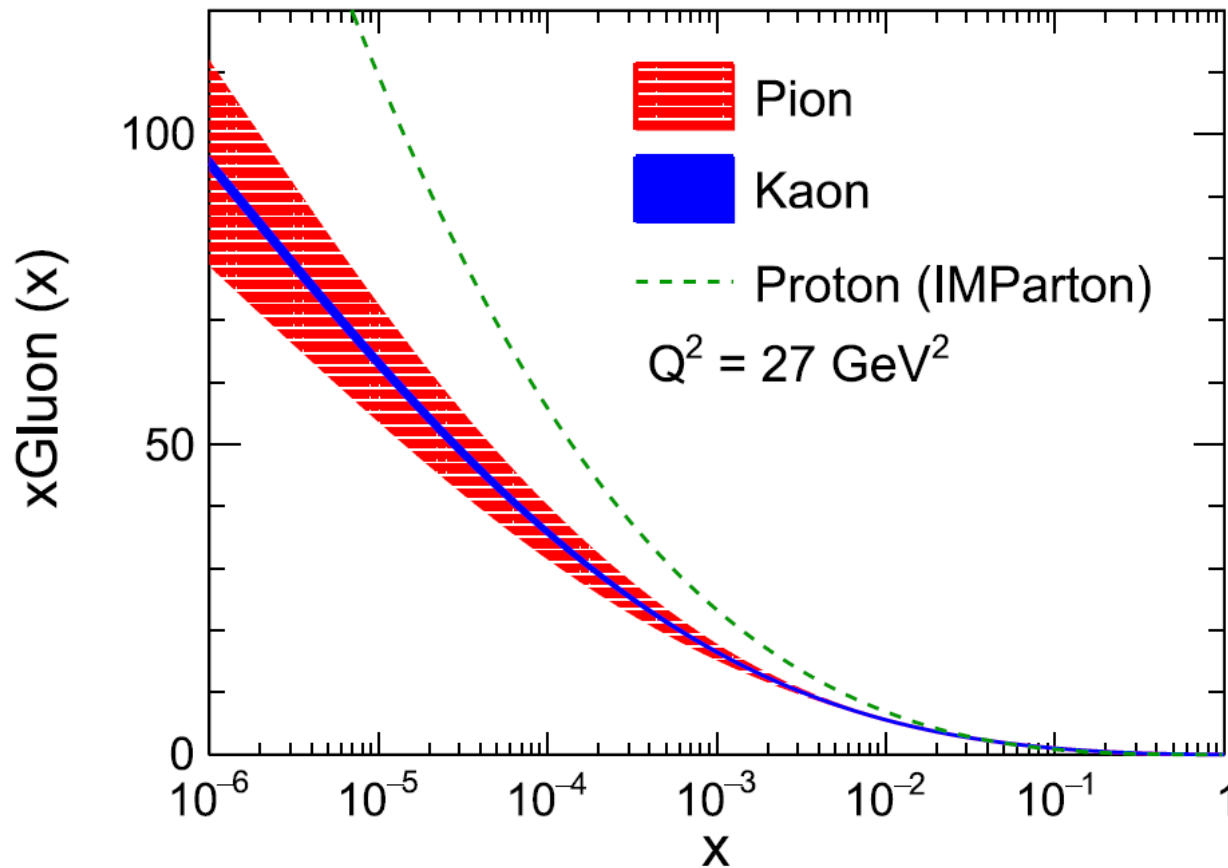
Kaon PDFs: Maximum Entropy Input

Eur. Phys. J. C (2021) 81:302



Kaon Gluon PDFs: Maximum Entropy Input

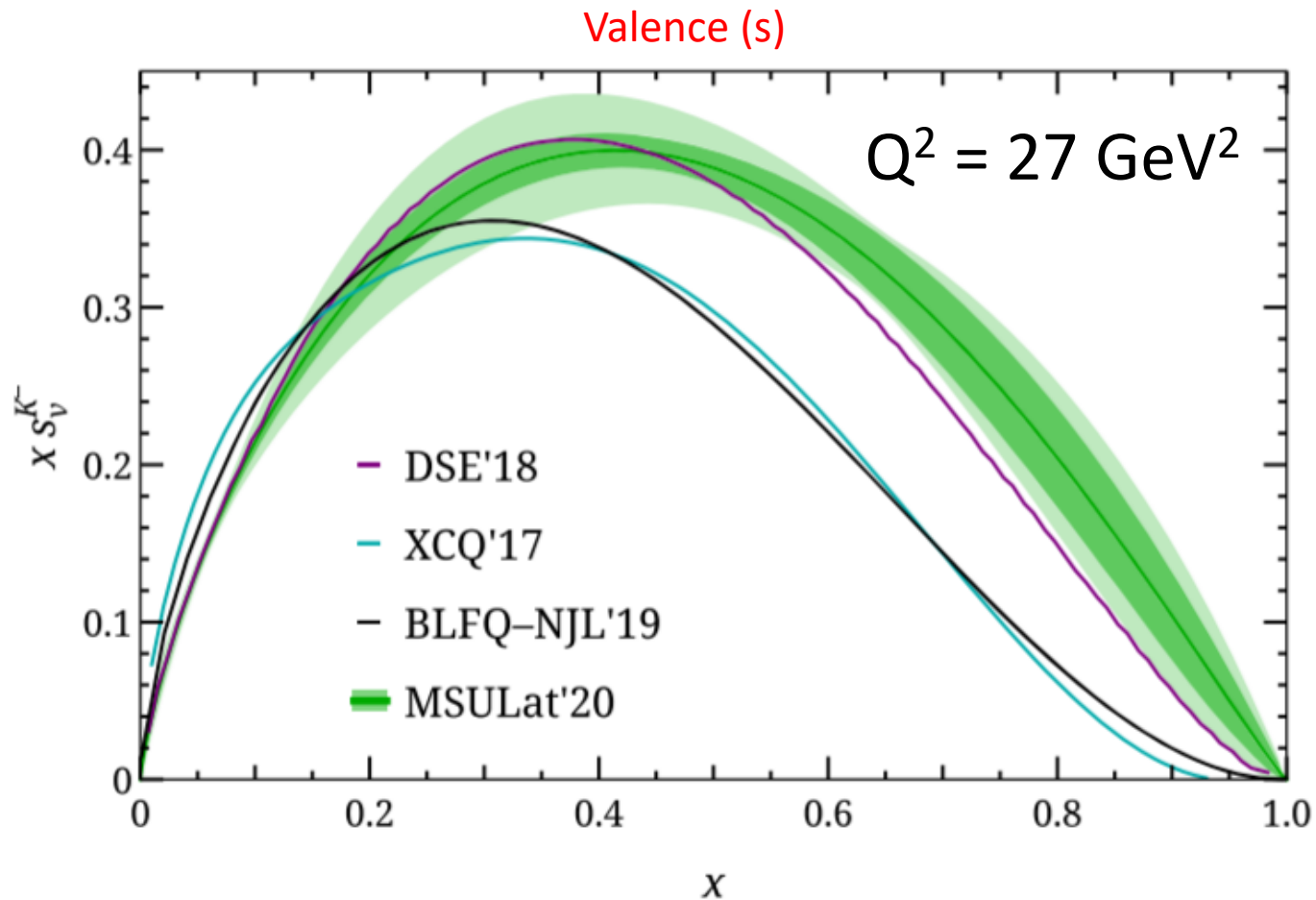
Eur. Phys. J. C (2021) 81:302



The gluon distributions of the pion and the kaon are quite similar

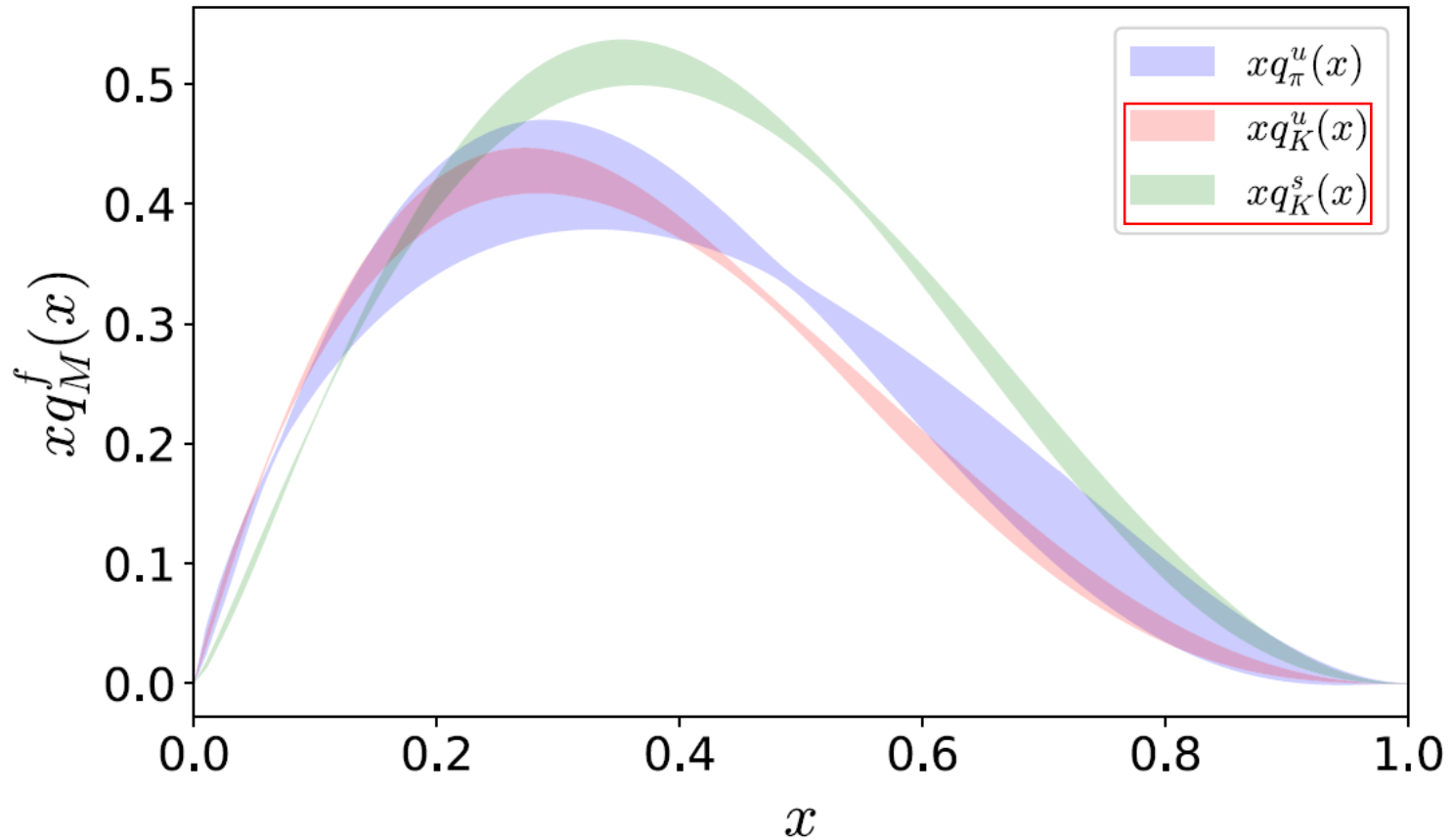
Kaon PDFs: LQCD(quasi-PDF)

PRD 103, 014516 (2021)



Kaon PDFs: LQCD (Mellin moments)

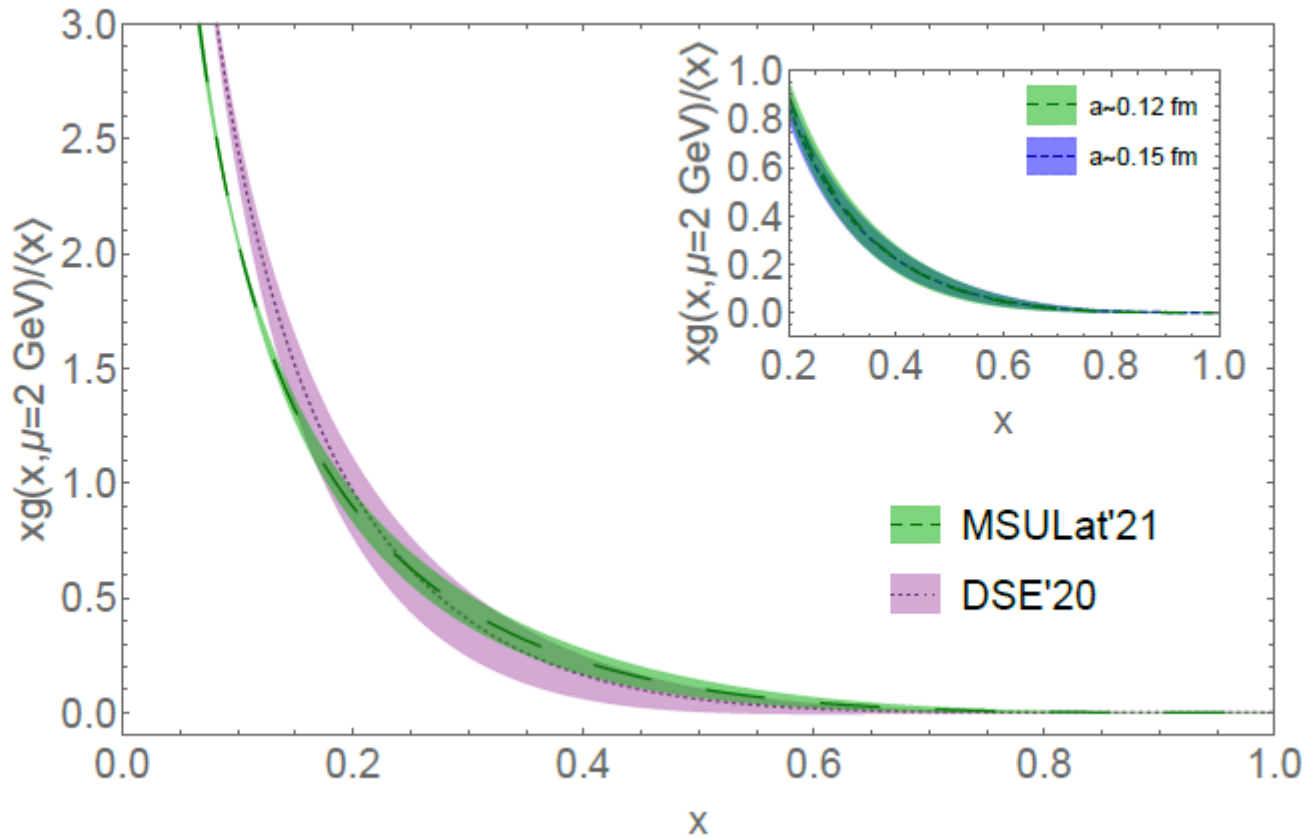
PRD 104, 054504 (2021)



Reconstructed by the lattice data up to $\langle x^3 \rangle$.

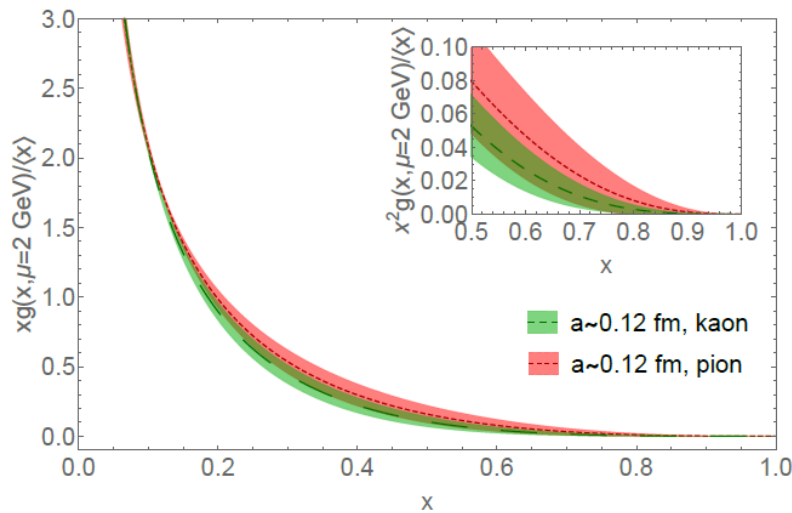
Kaon Gluon PDFs: LQCD(pseudo-PDF)

arXiv:2112.03124



(Reduced) Ioffe-time distributions, only the shape $xg/\langle x \rangle$ is predicted.

Gluon: Kaon vs. Pion



one-sigma error for $x > 0.15$. On the right-hand side of Fig. 5, we compare the obtained kaon result at smaller lattice spacing with the pion results obtained from the same ensembles; we note the kaon gluon PDF is slightly smaller than the one obtained for the pion, similar to its corresponding quark valence PDF and DSE [88] results. We predict the kaon $\langle x^2 \rangle_g / \langle x \rangle_g$ and $\langle x^3 \rangle_g / \langle x \rangle_g$ to be 0.0779(94) and 0.0187(42), while in good agreement with corresponding results from DSE [88]: 0.075 and 0.015. On the pion $\langle x^2 \rangle_g / \langle x \rangle_g$, our 310-MeV results gives .092(15) and 0.0250(75), while results from DSE [88], JAM [1, 2] and xFitter [3] are 0.076, 0.103, 0.158 and 0.015, 0.024, 0.048, respectively. Future study including finer lattice spacing and lighter pion mass will be important to refine this calculation and provide better predictions on this poorly known meson quantity.

A slightly smaller kaon gluon distribution at large x , compared to the pion.

CERN: COMPASS++/AMBER

Year >2026

Unique opportunities with RF separated beam

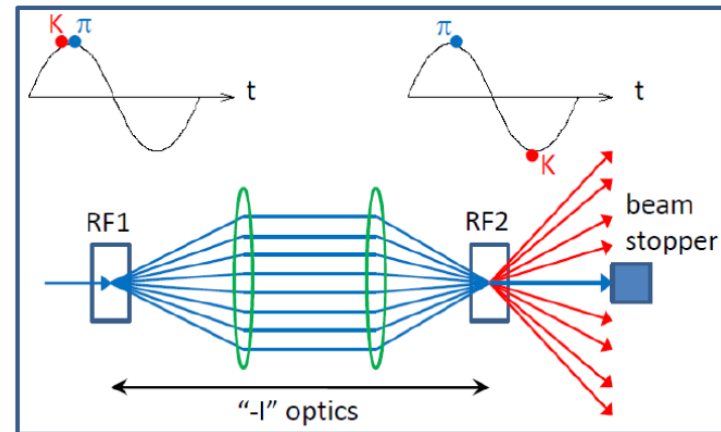
- Deflection with 2 cavities
- Relative phase = 0 \rightarrow dump
- Deflection of wanted particle given by
$$\Delta\phi \approx \frac{\pi f L}{c} \frac{m_w^2 - m_u^2}{p^2}$$

To keep good separation:

L should increase as p^2 for a given $f \rightarrow$ limits the beam momentum

Initial expectations before further R&D:

- ~ 80 GeV Kaon beam
- ~ 110 GeV Anti-proton beam

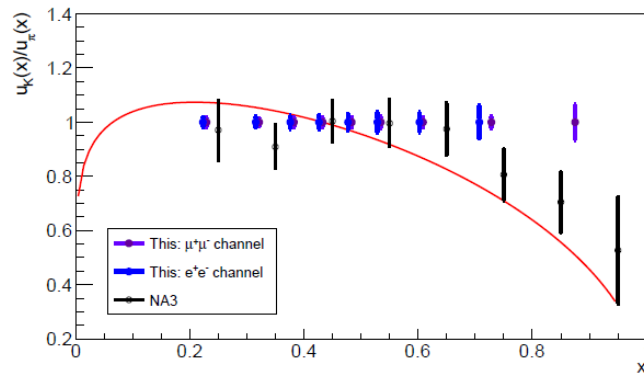


CERN: COMPASS++/AMBER

Year >2026

Projections for Kaon structure

140 days with $2 \times 10^7 \text{ s}^{-1}$ 100 GeV K^- beam:



Experiment	Target type	Beam type	Beam intensity (part/sec)	Beam energy (GeV)	DY mass (GeV/c ²)	DY events $\mu^+\mu^-$	
NA3	6 cm Pt	K^-		200	4.2 – 8.5	700	
This exp.	100 cm C	K^-	2.1×10^7	80	4.0 – 8.5	25,000	
				100	4.0 – 8.5	40,000	
				120	4.0 – 8.5	54,000	
This exp.	100 cm C	K^+	2.1×10^7	80	4.0 – 8.5	2,800	
				100	4.0 – 8.5	5,200	
				120	4.0 – 8.5	8,000	
This exp.	100 cm C	π^-	4.8×10^7	80	4.0 – 8.5	65,500	
					100	4.0 – 8.5	95,500
					120	4.0 – 8.5	123,600

π data taken simultaneously from beam impurity

Enlarge world data statistics by a factor 30

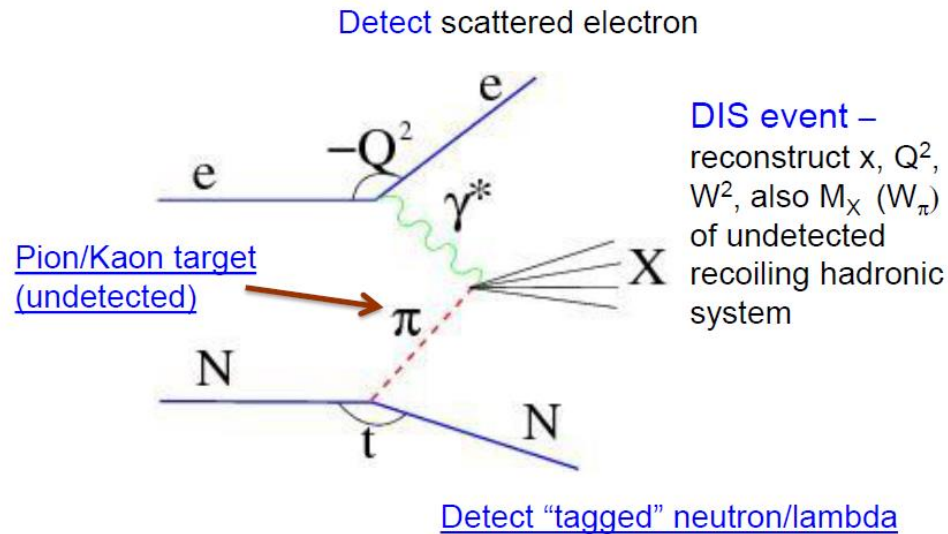
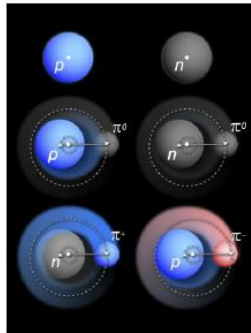
Determine u_K/u_π within a few percent

EIC: Tagged processes of DIS/Jpsi

Year >2030

Physics Objects for Pion/Kaon Structure Studies

- Sullivan process – scattering from nucleon-meson fluctuations

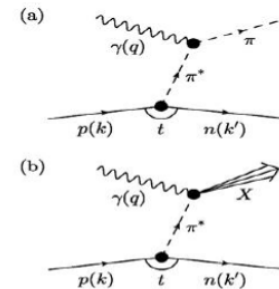
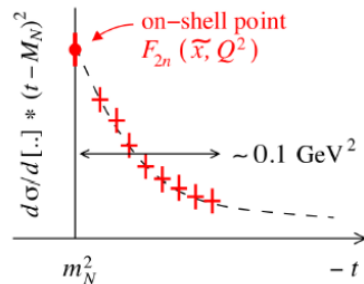


EIC: Sullivan Process

Year >2030

Pion and Kaon Sullivan Process

- The **Sullivan process can provide reliable access to a meson target** as t becomes space-like if the pole associated with the ground-state meson remains the dominant feature of the process and the structure of the related correlation evolves slowly and smoothly with virtuality.



- To **check these conditions** are satisfied empirically, one can **take data covering a range in t** and compare with phenomenological and theoretical expectations.

- Recent **theoretical calculations found that for $-t \leq 0.6 \text{ GeV}^2$, all changes in pion structure are modest** so that a well-constrained experimental analysis should be reliable. Similar analysis for the kaon indicates that Sullivan processes can provide a valid kaon target for $-t \leq 0.9 \text{ GeV}^2$.

[S.-X. Qin, C. Chen, C. Mezrag and C. D. Roberts, *Phys. Rev. C* **97** (2018) 015203.]

12

Summary

- Comparison of kaon and pion PDFs is important to explore the $SU(3)$ symmetry breaking effect.
- Data of kaon-induced Drell-Yan and J/ψ productions can be used to constrain the valence and gluon distributions. Nevertheless the data are scarce.
- Recent theoretical results of kaon PDFs show visible $SU(3)$ breaking effect in the valence distributions and the strength of gluon is slightly less, compared to pion.
- Data from the coming CERN AMBER and BNL EIC experiments will provide more data of constraining kaon PDFs.